pH-Controlled translocation of Ni^{II} within a ditopic receptor bearing an appended anthracene fragment: a mechanical switch of fluorescence

Valeria Amendola, Luigi Fabbrizzi,* Carlo Mangano, Piersandro Pallavicini, Angelo Perotti and Angelo Taglietti

Dipartimento di Chimica Generale, Università di Pavia, via Taramelli 12, I-27100 Pavia, Italy. Fax: +39 0382 507328; E-mail: fabbrizz@unipv.it

The sexidentate ligand **1** offers two distinct adjacent quadridentate coordinating compartments: a compartment B, consisting of two amine nitrogen atoms and two quinoline nitrogen atoms, and a poorly coordinating compartment AH$_2$, consisting of two amine nitrogen atoms and two amide nitrogen atoms, which, on deprotonation of the two amide groups, give the strongly coordinating donor set A^{2-}. Potentiometric and spectroscopic studies have shown that at pH = 7.5 the Ni^{II} ion stays in the B compartment (high-spin state, octahedral stereochemistry) and at pH $\geq$ 9.5, Ni^{II} is located in the adjacent A^{2-} compartment, as a low-spin centre, in a square stereochemistry. Thus, the Ni^{II} centre can be translocated from one compartment to the other by varying the pH from 7.5 to 9.5 and *vice versa*. The B-to-AH$_2$ translocation ($\tau = 0.25 \pm 0.01$ s) is faster than the reverse A^{2-}-to-B process ($\tau = 2.2 \pm 0.1$ s). When an anthracene (An) fragment is covalently linked to the AH$_2$ moiety (system **2**), the translocation of the Ni^{II} ion switches ON/OFF the An fluorescent emission, depending on whether the metal is positioned in the A^{2-} (OFF) or B compartment (ON). Quenching is due to a Ni^{II}-to-An* electron transfer process. Owing to steric hindrance of the bulky An substituent, both direct (B-to-AH$_2$, $\tau = 12 \pm 1$ s) and reverse (A^{2-}-to-B, $\tau = 66 \pm 12$ s) processes are distinctly slower than observed for system **1**.

Introduction

Bistable systems can be generated through the controlled movement of a mobile part of either a molecular or a supramolecular system, to give two topologically distinct forms.[1] When the system is dissolved in a solution, the motion can be induced by an external input like the variation of the redox potential or of the pH. Relevant examples include rotaxanes and catenanes.[2-8]

A situation of topological bistability can also be achieved by displacing an ionic particle, *e.g.* a metal ion, between two different sites of the same molecular receptor, following a predetermined route.[9] The driving force of the process may be a redox change involving the metal centre to be translocated. The two reported examples are associated with the Fe^{III}/Fe^{II} couple. In the first reported case, the iron centre has been made to move between two different compartments of a triple-stranded helical complex: a tris-hydroxamate donor set (compartment A) and a tris-2,2′-bipyridine set (compartment B).[10] When in the Fe^{III} state, the metal centre chooses A, but, when reduced to Fe^{II}, it moves to B. Then, the metal can be moved back to A, following chemical oxidation to the trivalent state. The process is thus reversible, but it is rather slow in view of the serious conformational changes experienced by the ditopic receptor during the translocation process. In a more recent example, the pendular motion of the iron centre between a soft compartment (suitable for Fe^{II} coordination) and a hard compartment (for Fe^{III}) of a ditopic receptor has been electrochemically triggered.[11] A redox input has also been used to translocate an anion between two metal centres within a heterodimetallic complex. In particular, a Cl$^-$ ion was reversibly translocated between a copper(II) and a nickel centre by using the Ni^{II}/Ni^{III} change as an engine.[12] Redox driven ion translocation represents another way to convert chemical energy into controlled motion, and the systems mentioned above can be considered the prototypes of a new class of molecular machines.

We describe here the design of a two-compartment receptor suitable for carrying out the translocation of a metal ion, driven by a change of pH. Owing to the great difference of the coordinating tendencies of the two compartments, the translocation process induces a drastic change of the electronic properties of the metal ion (Ni^{II}, from high-spin to low-spin), and is perceived through a change of the d–d absorption spectrum as well as of the colour. Moreover, when a photoactive fragment (anthracene, An) is covalently linked to one of the compartments, the pH controlled reversible translocation of the metal induces the consecutive quenching/revival of the An fluorescence, thus providing an example of a molecular-level light switch, which is mechanically operated.

Results and discussion

1. Design of the ditopic receptor

In order to allow the pH driven translocation of an M metal centre, the receptor should contain two distinct coordinating compartments, AH$_n$ and B. AH$_n$ is a Brønsted acid and possesses coordinating tendencies toward M much lower than B. However, its deprotonated form A^{n-} must be a much more powerful ligand than B. Thus, the ligating tendencies decrease along the sequence: A$^{n-} \gg$ B $\gg$ AH$_n$. In this situation, at lower pH values, the acidic compartment is in the AH$_n$ form and M prefers to stay in the B compartment. At higher pH values, AH$_n$ deprotonates and M moves to the more donating A^{n-} compartment. On acidification, AH$_n$ forms again and M moves back to compartment B. Thus, the metal centre can be repeatedly translocated back and forth between the two compartments by varying the pH within a narrow interval. The pH controlled translocation process is pictorially illustrated in Fig. 1.

The requirements outlined above can be fulfilled by the ligating system **1** which offers two distinct coordinating compartments: the compartment B is made of two amine nitrogen
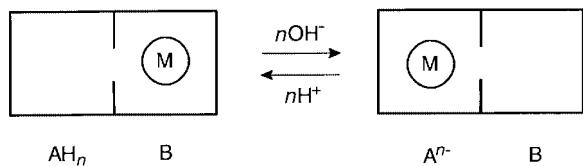
Fig. 1 The pH controlled translocation of a metal ion M between the two compartments of a heteroditopic ligand. AH_n is an n-protic acid and the coordinating affinity towards M decreases according to the sequence: $A^{n-} > B > AH_n$.

atoms and two quinoline nitrogen atoms. The other compartment, AH_2, consists of two amine nitrogen atoms and two amide nitrogen atoms: owing to the extremely scarce (or nil) donating tendencies of the amide groups, AH_2 is a very poor ligand. However, diamine–diamide chelating agents tend to coordinate divalent metal ions of the late 3d series (*e.g.* Ni^{II}), with simultaneous extrusion of two protons from the amide groups.[13] The doubly negatively charged donor set which forms is a very good ligand and establishes especially intense in-plane interactions. In particular, it is able to stabilize the low-spin state of Ni^{II}. Thus, the ditopic receptor **1** provides a compartment, AH_2, whose donor tendencies (i) can be drastically modified by a pH change (through the $AH_2 = A^{2-} + 2H^+$ acid–base equilibrium), and (ii) fit well the required sequence of affinity toward M (Ni^{II}): $A^{2-} > B > AH_2$.
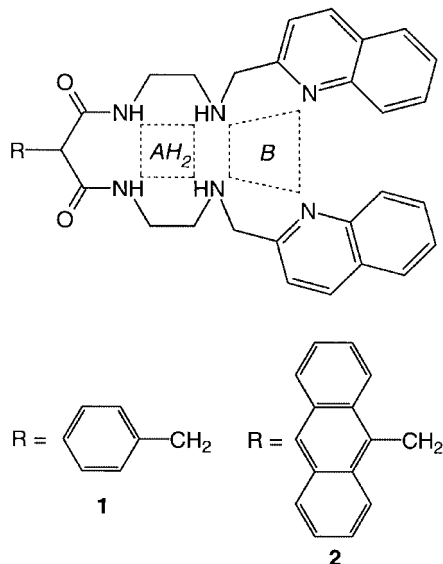
The central carbon atom of the trimethylenic chain linking the two amide nitrogen atoms is a synthetically convenient position to attach a desired functionality. In particular, in system **2** the photoactive anthracenyl fragment has been appended to the AH_2 compartment, with the aim of signalling the pH-driven movement of M from B to A^{2-}.

2. The pH driven reversible translocation of Ni^{II} within the ditopic receptor 1, studied by potentiometry and spectrophotometry

The coordinating tendencies of **1** toward Ni^{II} were investigated by carrying out potentiometric titration experiments on dioxane/water solution (4:1, v/v). Preliminary titration experiments were carried out on a solution containing system **1** alone, in order to determine the protonation constants. Then, a solution containing equimolar amounts of **1** (LH_2) and Ni^{II}, plus excess acid, was titrated with standard base. The equilibrium constants of the species that form over the investigated pH range (2–12) were calculated through a non-linear least-squares analysis of the titration curves,[14] and their values, which are reported in Table 1, were used to draw the distribution curves of the varying species.

Table 1 Logarithmic values of protonation constants and complex formation constants, for the systems ligand/Ni^{2+} in 1:1 molar ratio

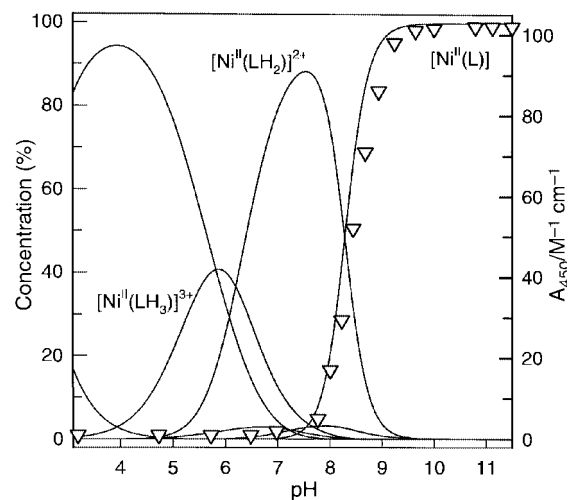| Equilibrium	1	2
$LH_2 + H^+ \rightleftharpoons [LH_3]^+$	7.25 ± 0.01	8.48 ± 0.02
$LH_2 + 2H^+ \rightleftharpoons [LH_4]^{2+}$	14.46 ± 0.01	15.50 ± 0.02
$LH_2 + 3H^+ \rightleftharpoons [LH_5]^{3+}$	16.87 ± 0.01	19.02 ± 0.02
$Ni^{2+} + LH_3^+ \rightleftharpoons [Ni^{II}(LH_3)]^{3+}$	4.77 ± 0.01	6.65 ± 0.03
$Ni^{2+} + LH_2 \rightleftharpoons [Ni^{II}(LH_2)]^{2+}$	5.83 ± 0.02	8.73 ± 0.04
$[Ni^{II}(LH_2)]^{2+} + 2OH^- \rightleftharpoons [Ni^{II}(L)] + 2H_2O$	12.42 ± 0.02	13.40 ± 0.04

Fig. 2 pH dependence of the percent concentration of the metal complex species for a solution 2×10^{-3} M in **1** (LH_2) and 2×10^{-3} M in Ni^{II} (dioxane/water 4:1 v/v; 0.1 M $NaClO_4$). Non indexed curves refer to the protonated species $[LH_{2+n}]^{n+}$ ($n = 1, 2, 3$). ∇ (right vertical axis) refer to the molar absorbance of the d–d band at 450 nm, pertinent to the low-spin $[Ni^{II}(L)]$ complex.

In particular, Fig. 2 illustrates the pH dependence of the concentration of the species present at equilibrium for a solution 5×10^{-3} M^{-1} both in **1** and in Ni^{II}. It is shown that two metal complex species prevail over the 6–12 pH interval: the complex of the neutral ligand, $[Ni^{II}(LH_2)]^{2+}$, and the complex of the doubly deprotonated ligand, $[Ni^{II}(L)]$. The $[Ni^{II}(LH_2)]^{2+}$ complex is present at 90% at pH = 7.5. The absorption spectrum of the solution adjusted at this pH, pale-blue in colour, displays two weak d–d bands centred at 606 nm ($\varepsilon = 11$ M^{-1} cm^{-1}) and 820 nm ($\varepsilon = 5$ M^{-1} cm^{-1}), typically observed with a high-spin Ni^{II} ion in an octahedral coordinative environment. Moreover, the mass spectrum (ESI) on a solution of $1/Ni^{2+}$ ($c = 5 \times 10^{-3}$ M), whose pH is adjusted to 7.5, demonstrates that $[Ni^{II}(LH_2)]^{2+}$ is a monomeric species (main peaks at 617, 619, $[LH_2 + Ni - H]^+$; 717, 719, $[LH_2 + Ni + ClO_4]^+$). In this species, the amide groups are not deprotonated, and due to their very poor binding tendencies, a coordination of Ni^{II} by compartment A seems to be excluded. It is therefore suggested that in the $[Ni^{II}(LH_2)]^{2+}$ form the metal centre stays in compartment B, being coordinated by the two amine and two quinoline nitrogen atoms, which in this species are not protonated. The coordination by the quinoline fragments is supported by the fact that the weak emission band of quinoline (392 nm) is quenched on Ni^{II} coordination, *i.e.* on going from pH 5.5 to 7.5. Two water molecules probably occupy the two vacant positions of a distorted octahedron, either in *cis* or *trans* position.

On increasing pH, the concentration of $[Ni^{II}(LH_2)]^{2+}$ decreases, whereas the $[Ni^{II}(L)]$ complex begins to form, to reach 100% at pH ≥ 9.5. At the same time, the solution takes on a bright yellow colour and a band develops at 450 nm ($\varepsilon = 103$ M^{-1} cm^{-1}). Such a band is typically observed with the square-planar low-spin Ni^{II} complexes of bis-deprotonated diamino–diamido open chain ligands, and has to be associated with the
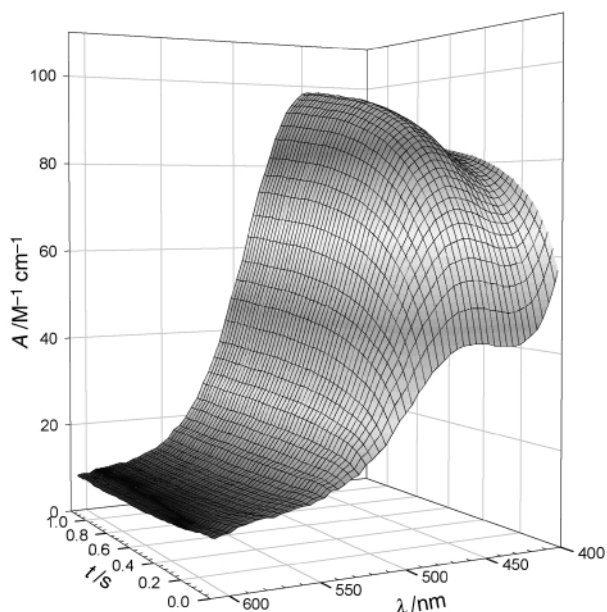
Fig. 3 The family of spectra recorded on a diode array spectrophotometer after the mixing of a solution of $[Ni^{II}(LH_2)]^{2+}$ (pH = 7.5) with a solution buffered at pH = 9.5. Spectra from which the surface originated were taken every 25 ms.

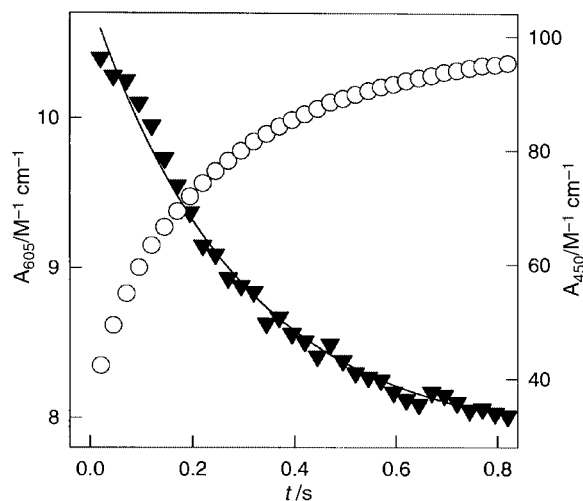**Fig. 4** Temporal profiles of the molar absorbance of the bands: at 450 nm (○), and at 605 nm (▼), after the mixing of a solution of $[Ni^{II}(LH_2)]^{2+}$ (pH = 7.5) with a solution buffered at pH = 9.5, in a stopped-flow unit.

$[Ni^{II}(L)]$ form, in which the metal centre occupies the A^{2-} compartment and is present in its low-spin form, as confirmed also by mass spectra (ESI, main peaks at 617, 619, $[L + Ni + H]^+$). In particular, it is observed in Fig. 2 that the profile of the molar absorbance of the yellow low-spin chromophore vs. pH superimposes well on the curve of the concentration of the $[Ni^{II}(L)]$ species. Thus, a pH change from 7.5 (dominant species: $[Ni^{II}(LH_2)]^{2+}$) to 9.5 (dominant species: $[Ni^{II}(L)]$) induces the translocation of the Ni^{II} centre from compartment B to compartment A^{2-} of the ditopic receptor **1**: the intramolecular motion is visually perceived through the colour change of the solution from pale blue to bright yellow, which is due to the occurrence of a drastic electronic rearrangement (the Ni^{II} high-spin/low-spin crossover).

Noticeably, the progress of the metal translocation process can be followed through a stopped-flow spectrophotometric experiment. In particular, when an aqueous ethanolic solution of $[Ni^{II}(LH_2)]^{2+}$ (pH = 7.5) is mixed with an aqueous ethanolic solution buffered at pH = 9.5, a band at 450 nm develops and reaches a plateau within less than one second. The temporal
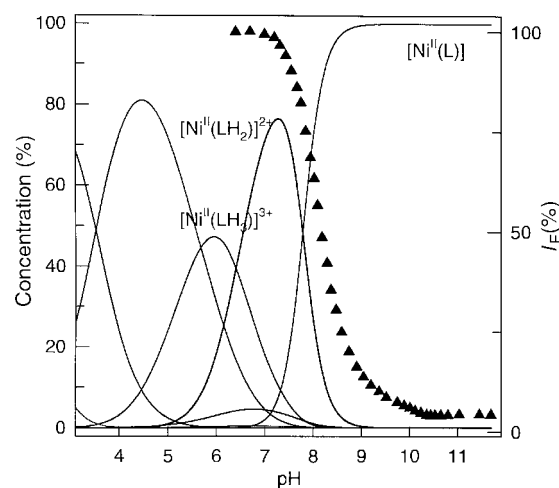

Fig. 5 pH dependence of the percent concentration of the metal complex species for a solution 2×10^{-5} M in **2** (LH_2) and 2×10^{-5} M in Ni^{II} (dioxane/water 4:1 v/v; 0.1 M NaClO$_4$). Non indexed curves refer to the protonated species $[LH_{2+n}]^{n+}$ ($n = 1, 2, 3$). ▲ (right vertical axis) indicate the intensity of the fluorescence emission, I_F, for the same solution, when varying pH.

development of the band pertinent to the $[Ni^{II}(L)]$ complex is illustrated in Fig. 3. The profile of the increasing molar absorbance of the band at 450 nm is shown in Fig. 4: the process is first-order, with a lifetime of 0.25 ± 0.01 s. The translocation process can also be followed through the decay of the band at 606 nm, associated with the high-spin $[Ni^{II}(LH_2)]^{2+}$ complex (see Fig. 4). The lifetime of the first order decay ($\tau = 0.26 \pm 0.04$ s) is coincident, within experimental error, with that associated with the formation of the $[Ni^{II}(L)]$ complex.

On the other hand, when the pH of the yellow solution containing $[Ni^{II}(L)]$ (pH $\geq$ 9.5) is brought back to 7.5, the pale blue colour is quickly restored, indicating that the metal has been translocated again to the B compartment. Back translocation was followed by stopped-flow techniques through the mono-exponential decrease of the intensity of the band at 450 nm and is considerably slower than the B to AH_2 translocation ($\tau = 2.2 \pm 0.1$ s). The distinctly different rates of the two processes can be mainly ascribed to the fact that B-to-AH_2 translocation involves the dissociation of a high-spin Ni^{II} ion, whereas A^{2-}-to-B translocation involves the dissociation of a low-spin Ni^{II} cation: it is well known that d^8 low-spin metal centres, in a square-planar coordinative arrangement, are particularly inert with respect to ligand substitution, due to the high value of the ligand field activation energy.[15]

3. The pH driven reversible translocation of Ni^{II} within the ditopic receptor 2, studied by potentiometry and spectrofluorimetry

Having ascertained that the framework of receptor **1** is especially convenient for carrying out pH-driven metal translocation processes, we equipped it with a powerful photoactive fragment. In particular, the phenyl ring linked to the AH_2 compartment of **1** was replaced by an anthracenyl substituent, to give **2**.

Potentiometric titration experiments indicated that the same species observed for system **1** are present at equilibrium over the 2–12 pH range, in a dioxane/water solution (4:1, v/v) containing equimolar amounts of **2** and Ni^{II} (see Table 1 for formation constants). In particular, the $[Ni^{II}(LH_2)]^{2+}$ species shows its maximum concentration at pH = 7.5, while the other major species, $[Ni^{II}(L)]$, is present at 100% at pH $\geq$ 9.5 (see the distribution diagram in Fig. 5).[16] Thus, also in the case of system **2**, the Ni^{II} ion can be moved back and forth between the two compartments by simply varying the pH from 7.5 to 9.5 and vice versa. However, the translocation processes cannot be monitored satisfactorily spectrophotometrically, as the band of the

[Ni^{II}(L)] form is obscured in part by the strong anthracene absorption and is observed only as a shoulder at 420 nm. However, both direct and reverse translocation can be followed by spectrofluorimetry. In particular, a water/dioxane solution containing equimolar amounts of **2** and Ni^{II} was titrated with standard base inside the spectrofluorimetric cuvette. The intensity of the anthracene (An) emission, I_F, whose values are superimposed on the distribution diagram in Fig. 5, shows its highest value at pH = 7.5, *i.e.* corresponding to the [Ni^{II}-(LH$_2$)]$^{2+}$ species. The emission intensity of the solution of the [Ni^{II}(LH$_2$)]$^{2+}$ complex is the same as that of a solution of **2** in the absence of metal at the same pH, and comparable to that of unsubstituted anthracene under the same conditions. This indicates that the Ni^{II} centre, when in the B compartment, is far enough away from the An fluorophore to not interfere with its radiative decay, a phenomenon well set in what has been recorded in the literature regarding the efficiency of the quenching processes as a function of the fluorophore–quencher distance.[17] As the pH increases, I_F decreases following a sigmoidal profile, to complete fluorescence quenching at pH ≥ 9.5, where 100% of the [Ni^{II}(L)] form is present (see Fig. 5). Thus, the position of the Ni^{II} centre within system **2** is sharply signalled by the emission of the anthracene component: when the metal is in compartment B, fluorescence is ON; when it is in compartment A^{2-}, fluorescence is OFF. It has been previously shown that a Ni^{II} ion, when coordinated by a deprotonated diamide–diamine donor set, quenches a methylene linked anthracene fragment through a metal-to-fluorophore electron transfer (eT) mechanism, a process made possible by the easy oxidation to Ni^{III} in that coordinative environment.[18] It should also be noted that the occurrence of a Ni^{II}-to-An* electron transfer (eT) process is fully accounted for on a thermodynamic basis. In particular, the ΔG°_{eT} value is distinctly negative (-0.35 eV), as calculated from the appropriate combination of the pertinent photophysical ($E^{0-0} = -3.1$ eV) and electrochemical quantities (eE°(Ni^{III}/Ni^{II}; e is the electronic charge) = 0.35 eV; eE°(An/An$^-$) = -2.4 eV).[18] Thus, it is suggested that, when in the A^{2-} compartment, the Ni^{II} centre quenches the nearby An* fragment through a metal-to-fluorophore eT process. When, following acidification to pH = 7.5, the metal is removed from the A^{2-} compartment and brought back to the B compartment, the eT mechanism vanishes and fluorescence is restored. The translocation processes, both direct and reverse, can be temporally followed, this time by carrying out spectrofluorimetric stopped-flow experiments and by monitoring the first order decay-development of I_F. The B-to-AH$_2$ translocation ($\tau = 12 \pm 1$ s) is faster than A^{2-}-to-B back translocation ($\tau = 66 \pm 12$ s), as observed with system **1**. However, the rates of both direct and reverse processes are remarkably slower for **2** than for **1**. This may be due to the presence of the bulky anthracene substituent which slows down the conformational rearrangement experienced by the ligating backbone during translocation. In particular, metal translocation may be associated with the occasional folding of the ditopic receptor (**1** or **2**) around the ideal line joining the two amine nitrogen atoms, which acts as a hinge. It is suggested that the transition state for the translocation process corresponds to a situation of maximum folding, in which the two halves of the receptor are brought face to face at the closest possible distance, an event which precedes the metal transfer. It seems reasonable that the bulky anthracene substituent raises the energy of such a transition state, thus slowing down the rate of both direct and reverse translocation processes.

Finally, it has to be noted that although many molecular switches have been described,[19] in which the emitting properties of a fluorescent component can be turned ON/OFF in solution by the variation of an external parameter (applied redox potential, pH), in most cases the reported examples deal with *static* molecular systems: *e.g.* on changing the oxidation state of a coordinated metal cation,[20] or on protonation of an amino group[19,21] it is possible to switch ON/OFF (or *vice versa*) the fluorophore emission inside two-component *fixed* molecular systems. On the other hand, very few systems have been reported in which the *movement* of a fragment with respect to the whole molecule induces strong variations in the emission of a fluorescent component.[22] System **2**/Ni^{2+} is a new example of this kind of system, which can be considered *dynamic* switches of fluorescence: the light emission can be repeatedly turned ON/OFF by moving a component (the metal ion) back and forth, from one definite position to another. Interestingly, this provides a close analogy to the electromechanical light switches of the macroscopic world (in which a device, following an external stimulus, *e.g.* the pressure of a finger, turns ON/OFF repeatedly, at will, the light emitted by a bulb, linked through an electrical wire). In this context, it is worthwhile to remark that the switching device described here, which is operated through the consecutive additions of fractions of a drop of standard acid or base (enough to change the pH from 7.5 to 9.5 and *vice versa*), displays the properties typically required for an electromechanical switch: efficiency, reversibility, resistance to fatigue.

Experimental

Synthesis

The synthetic route to the receptors **1** and **2** is illustrated in Scheme 1. The dioxotetramines with an appended benzyl or 9,10-anthracenyl group were prepared by reaction of a large excess of ethylenediamine with 6-benzyl-1,4,8,11-tetraazaundecane-5,8-dione or 6-(anthracen-9-ylmethyl)-1,4,8,11-tetraazaundecane-5,8-dione, respectively, as previously described.[16] 2-Quinolinecarbaldehyde was purchased from Aldrich and used as such.

Receptor 1. A solution of 2-quinolinecarbaldehyde (0.34 g, 2.16 mmol) in 10 mL ethanol was added dropwise to a solution
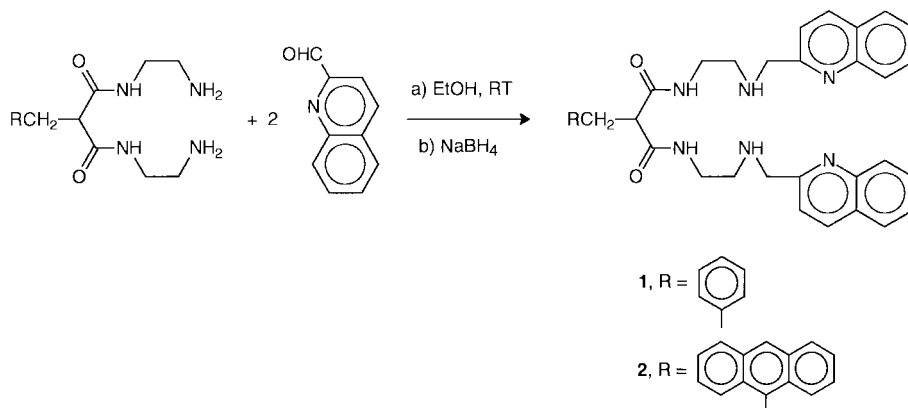
Scheme 1 The synthetic route to **1** and **2**.

of 5-benzyl-1,4,8,11-tetraazaundecane-5,8-dione (0.30 g, 1.08 mmol) in 30 mL ethanol, at room temperature. The bis-imino quinoline derivative precipitated after a few minutes as a white solid, which was collected by filtration and washed with some drops of chilled ethanol; the solid (0.3 g) was reduced with excess $NaBH_4$ in refluxing ethanol (50 mL). Evaporation of the solvent, treatment with excess water and extraction with CH_2Cl_2 allowed the recovery of pure ligand **1** as a white solid (75% yield), for which correct elemental analysis (Calc. for $C_{34}H_{36}N_6O_2$: C, 72.87; H, 6.42; N, 14.99; found: C, 72.95; H, 6.44; N, 14.96%) was found. Mass (ESI) 561 (M + H^+). NMR (CDCl$_3$): δ 8.10 (d, 2H), 8.02 (d, 2H), 7.78 (d, 2H), 7.69 (t, 2H), 7.50 (t, 2H), 7.39 (d, 2H) H of the quinoline rings; 7.2 (m, 5H, benzene ring); 7.11 (broad t, 2H, -CO-NH-); 4.0 (s, 4H, NH-CH_2-quinoline); 3.35 (m, 4H, CONH-CH$_2$-CH_2-); 3.2 (m, 3H, bz-CH_2-CH); 2.8 (m, 4H, CONH-CH_2-CH$_2$); 1.8 (broad, CH$_2$-NH-CH$_2$).

Receptor 2. This was prepared using a slight modification of the procedure described above: the bis-imino quinoline derivative was not isolated, but reduced *in situ* and the obtained final product was a dense yellow oil. Yield 55%. Mass (ESI): 661 (M + H$^+$). NMR (CDCl$_3$): δ 8.4–7.1 (m, 23H; H of the anthracene and quinoline rings + -CO-NH-); 4.2 (s, 4H, NH-CH_2-quinoline); 3.45 (t, 4H, CONH-CH$_2$-CH_2-); 3.15 (m, 3H, bz-CH_2-CH); 2.6 (m, 4H, CONH-CH_2-CH$_2$); 1.8 (broad, CH$_2$-NH-CH$_2$).

Equilibrium and stopped-flow studies

The protonation and Ni^{II} complex formation equilibria of **1** and **2** were studied in a dioxane/water solution (4:1 v/v), 0.1 M NaClO$_4$ at 25 °C, by titrating with standard base a solution containing **1** (or **2**) and excess strong acid (to determine protonation constants), and a solution containing **1** (or **2**), 1 equiv. of Ni^{II}(ClO$_4$)$_2$ plus excess acid (to determine the complex formation constants). Potentiometric studies were carried out using the fully automated unit described previously.[23] The titration curves were fitted and the equilibrium constants were calculated using the non-linear least-squares program HYPERQUAD.[14]

Absorption spectra were taken on a Hewlett-Packard 8452A spectrophotometer; emission spectra were recorded on a Perkin-Elmer Luminescence Spectrometer LS 50B. Spectrophotometric kinetic studies were carried out by using a stopped-flow system coupled to a diode array J&M TIDAS spectrophotometer, as previously described.[24] Spectrofluorimetric stopped-flow studies were carried out using a Hi-Tech SFA Rapid Kinetics Accessory unit coupled to the spectrofluorimeter. In a typical experiment, one syringe of the stopped-flow apparatus contained a metal complex solution (4 × 10^{-3} M for spectrophotometry; 2 × 10^{-5} M for spectrofluorimetry), adjusted to the desired pH with standard acid or base, while the other syringe contained a solution buffered to the desired pH value with HEPES (for pH = 7.5) or CHES (for pH = 9.5) buffer.

Spectrophotometric kinetic studies could not be carried out in the dioxane/water medium, as dioxane tends to dissolve the O-rings present in the stopped-flow unit, thus were performed in an ethanol/water mixture (4:1 v/v), 0.05 M in NaClO$_4$, at 25 °C. Potentiometric studies indicated that the same species observed in dioxane/water were present in ethanol/water and their distribution curves were found to be coincident with those reported in Fig. 2. The only point is that, probably due to some instability of the glass electrode in an ethanol-containing solution, the log K values thus obtained were affected by large uncertainties. Very importantly, the spectra of the solutions containing an equimolar amount of **1** and Ni^{II} in the two investigated media are coincident for both wavelength and molar absorbance, over the 6–12 pH range.

References

1 J.-M. Lehn, *Supramolecular Chemistry, Concepts and Perspectives*, VCH, Weinheim, 1995, pp. 124–127.
2 A. Livoreil, C. O. Dietrich-Buchecker and J.-P. Sauvage, *J. Am. Chem. Soc.*, 1994, **116**, 9399.
3 J.-P. Collin, P. Gaviña, P. V. Heitz and J.-P. Sauvage, *Eur. J. Inorg. Chem.*, 1998, **1**, 1.
4 M. Akasawa, P. R. Ashton, V. Balzani, A. Credi, C. Hamers, C. Mattersteig, M. Montalti, L. Prodi, L. A. N. Shipway, N. Spencer, J. F. Stoddart, M. S. Tolley, M. Venturi, A. J. P. White and D. J. Williams, *Angew. Chem., Int. Ed.*, 1998, **37**, 333.
5 R. A. Bissell, E. Córdova, A. E. Kaifer and J. F. Stoddart, *Nature (London)*, 1994, **369**, 133.
6 P. R. Ashton, R. Ballardini, V. Balzani, I. Baxter, A. Credi, M. C. T. Fyfe, M. T. Gandolfi, M. Gómez-López, M.-V. Martinez-Diaz, A. Piersanti, N. Spencer, J. F. Stoddart, M. Venturi, A. J. P. White and D. J. Williams, *J. Am. Chem. Soc.*, 1998, **120**, 11932.
7 V. Balzani, M. Gómez-López and J. F. Stoddart, *Acc. Chem. Res.*, 1998, **31**, 405.
8 J.-P. Sauvage, *Acc. Chem. Res.*, 1998, **31**, 611.
9 Ref. 1, pp. 134–135.
10 L. Zelikovich, J. Libman and A. Shanzer, *Nature (London)*, 1995, **374**, 790.
11 C. Belle, J.-L. Pierre and E. Saint-Aman, *New J. Chem.*, 1998, **22**, 1399.
12 L. Fabbrizzi, F. Gatti, P. Pallavicini and E. Zambarbieri, *Chem. Eur. J.*, 1999, **5**, 682.
13 L. Fabbrizzi, T. A. Kaden, A. Perotti, B. Seghi and L. Siegfried, *Inorg. Chem.*, 1986, **25**, 321.
14 A. Sabatini, A. Vacca and P. Gans, *Coord. Chem. Rev.*, 1992, **120**, 389.
15 F. Basolo and R. G. Pearson, *Mechanisms of Inorganic Reactions*, Wiley, New York, 1967.
16 Also in this case, mass spectra (ESI) measured on solutions adjusted to pH 7.5 (main peaks at 717, 719 [LH$_2$ + Ni − H]$^+$; 817, 819 [LH$_2$ + Ni + ClO$_4$]$^+$) and 9.5 (main peaks at 717, 719 [L + Ni + H]$^+$) indicate that the [Ni^{II}(LH$_2$)]$^{2+}$ and [Ni^{II}(L)] species are monomeric.
17 (*a*) M. N. Paddon-Row, *Acc. Chem. Res.*, 1994, **27**, 18; (*b*) A. P. de Silva, H. Q. N. Gunaratne and C. P. McCoy, *Chem. Commun.*, 1996, 2399; (*c*) L. Fabbrizzi, F. Gatti, P. Pallavicini and L. Parodi, *New J. Chem.*, 1998, **22**, 1403.
18 L. Fabbrizzi, M. Licchelli, P. Pallavicini, A. Perotti, A. Taglietti and D. Sacchi, *Chem. Eur. J.*, 1996, **2**, 75.
19 L. Fabbrizzi and A. Poggi, *Chem. Soc. Rev.*, 1995, **24**, 197.
20 (*a*) G. De Santis, L. Fabbrizzi, M. Licchelli, C. Mangano and D. Sacchi, *Inorg. Chem.*, 1995, **34**, 3581; (*b*) G. De Santis, L. Fabbrizzi, M. Licchelli, N. Sardone and A. H. Velders, *Chem. Eur. J.*, 1996, **2**, 1243.
21 (*a*) A. P. de Silva and R. A. D. D. Rupasinghe, *J. Chem. Soc., Chem. Commun.*, 1985, 1669; (*b*) A. P. de Silva, H. Q. N. Gunaratne, T. Gunnlaugsson, A. J. M. Huxley, C. P. McCoy, J. T. Rademacher and T. E. Rice, *Chem. Rev.*, 1997, **97**, 1515.
22 L. Fabbrizzi, M. Licchelli, P. Pallavicini and L. Parodi, *Angew. Chem., Int. Ed.*, 1998, **37**, 800.
23 V. Amendola, L. Fabbrizzi, P. Pallavicini, L. Parodi and A. Perotti, *J. Chem. Soc., Dalton Trans.*, 1998, 2053.
24 G. De Santis, L. Fabbrizzi, A. Perotti, N. Sardone and A. Taglietti, *Inorg. Chem.*, 1997, **36**, 1998.

Paper a907966a